LUND UNIVERSITY

A Sequel to: Analytical and Experimental Investigation of Stability of Frames and Arches Subjected to Follower Forces

Arif, Ghazi Majid

1991

Link to publication

Citation for published version (APA):
Arif, G. M. (1991). *A Sequel to: Analytical and Experimental Investigation of Stability of Frames and Arches Subjected to Follower Forces*. (LUTVDG/TVBB--3062--SE; Vol. 3062). Department of Fire Safety Engineering and Systems Safety, Lund University.

Total number of authors:
1

General rights
Unless other specific re-use rights are stated the following general rights apply:
Copyright and moral rights for the publications made accessible in the public portal are retained by the authors and/or other copyright owners and it is a condition of accessing publications that users recognise and abide by the legal requirements associated with these rights.
• Users may download and print one copy of any publication from the public portal for the purpose of private study or research.
• You may not further distribute the material or use it for any profit-making activity or commercial gain
• You may freely distribute the URL identifying the publication in the public portal

Read more about Creative commons licenses: https://creativecommons.org/licenses/

Take down policy
If you believe that this document breaches copyright please contact us providing details, and we will remove access to the work immediately and investigate your claim.

LUND UNIVERSITY

PO Box 117
221 00 Lund
+46 46-222 00 00

LUND UNIVERSITY · SWEDEN
INSTITUTE OF TECHNOLOGY
DEPARTMENT OF FIRE SAFETY ENGINEERING
CODEN: SE–LUTVDG/TVBB–3062
ISSN 0284–933X

GHAZI MAJID ARIF

A SEQUEL TO: ANALYTICAL AND EXPERIMENTAL INVESTIGATION OF STABILITY OF FRAMES AND ARCHES SUBJECTED TO FOLLOWER FORCES

Lund, August, 1991

Introduction

The displacement method developed for the analysis of the stability of circular arches in paper (1) excludes the mass of the arch. To overcome the short-comings of paper (1) in this respect, the method of initial parameters is employed below in the derivation of the frequency equations of a circular arch subjected to a nonconservative follower force Q at the free end (Figs 1, 2) and taking into account the mass of the arch.

1. Equations of motion

The differential equation of vibration of a circular arch, with mass density m, subjected to uniform pressure intensity p, perpendicular to the arch, is

$$\frac{\partial^6 \overline{w}}{\partial \theta^6} + (1 + \nu^2) \frac{\partial^4 \overline{w}}{\partial \theta^4} + (\nu^2 - u^4) \frac{\partial^2 \overline{w}}{\partial \theta^2} + u^4 \overline{w} = 0 \tag{1}$$

where

$$\nu^2 = 1 + \frac{pR^3}{EI}$$
$$u^4 = \frac{m\omega^2 R^4}{EI} \tag{2}$$

For notations, see appendix (1).

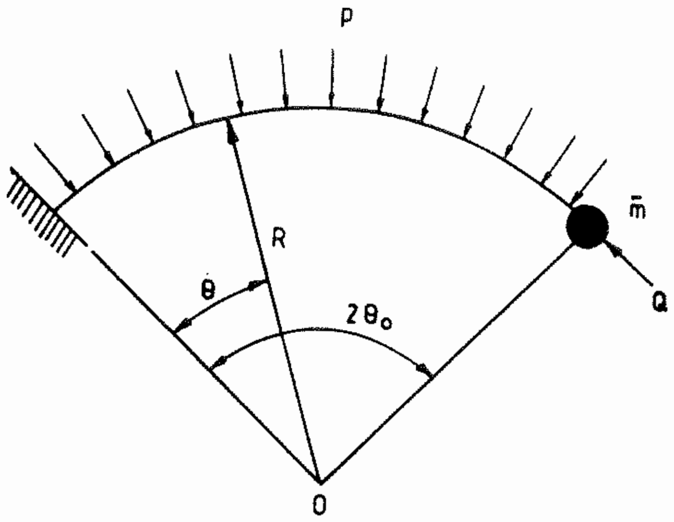

Fig. 1 Fixed–free arch

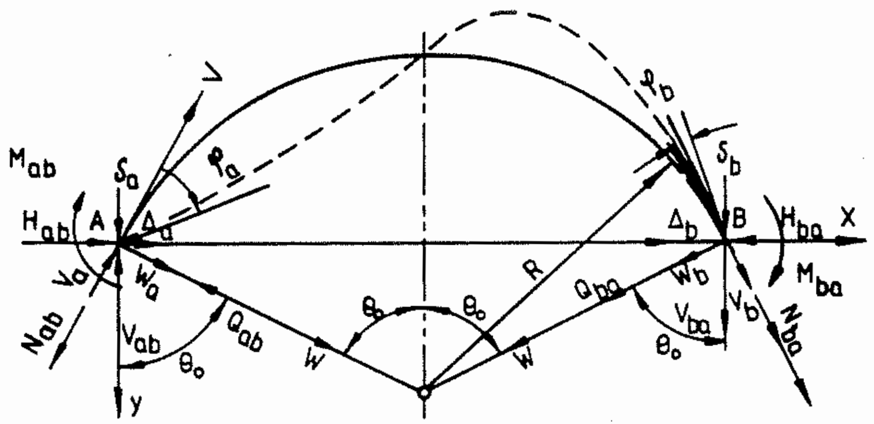

Fig. 2 Member end displacements and forces of a circular arch

By expressing a solution in the form $\overline{w}\ (x,t) = w(x)\ e^{i\lambda t}$, the characteristic equation of (1) is as follows

$$\lambda^6 + (1+\nu^2)\ \lambda^4 + (\nu^2-u^4)\ \lambda^2 + u^4 = 0 \tag{3}$$

Changing equation (3) to a cubic form by setting $\lambda^2 = y$, we have

$$y^3 + (1+\nu^2)\ y^2 + (\nu^2-u^4)\ y + u^4 = 0 \tag{4}$$

The following relations are derived

$$\lambda_3^2 = \frac{(1 + \lambda_1^2)\ (1 + \lambda_2^2)}{2\lambda_1^2\ \lambda_2^2 - (1 + \lambda_1^2)\ (1 + \lambda_2^2)}$$

$$\nu^2 = -\ (\lambda_1^2 + \lambda_2^2 + \lambda_3^2) - 1$$

$$u^4 = -\ \lambda_1^2\ \lambda_2^2\ \lambda_3^2 \tag{5}$$

where $y_1 = \lambda_1^2$, $y_2 = \lambda_2^2$, $y_3 = \lambda_3^2$ are the roots of equation (4).

The roots of the characteristic equation (3) have the following properties

1) If $a^3 > b^2$ then $(\lambda_1^2$ and $\lambda_2^2)$ are real and different
2) If $a^3 = b^2$ then $(\lambda_1^2 = \lambda_2^2)$ are two real and equal roots
3) If $a^3 < b^2$ then $(\lambda_1^2$ and $\lambda_2^2)$ are complex roots

where a and b are given as

$$a = \frac{(1 + \nu^2)^2}{9} - \frac{\nu^2 - u^4}{3} \tag{6}$$

$$b = \frac{(1 + \nu^2)^3}{27} - \frac{(1 + \nu^2)\ (\nu^2 - u^4)}{6} + \frac{u^4}{2}$$

2. Stability analysis

Consider the vibration of the circular arch, assuming elastic supports at the ends A and B, then the deflections, moments and shear equations are as follows

$$M_{ab} = -\ C_a^{\varphi}\ \varphi_a$$

$$Q_{ab} = C_a^{w}\ w_a$$

$$N_{ab} = -\ C_a^{v}\ v_a \tag{7}$$

$$M_{ba} = - C_b^{\varphi} \varphi_b$$
$$Q_{ba} = C_b^{w} w_b$$
$$N_{ba} = - C_b^{NC} \varphi_b - C_b^{v} v_b$$

where

$$C_b^{NC} = - \frac{v^2}{\cos\theta_o}; \; C_b^{\varphi} = C_o$$
$$C_b^{v} = k_1 + u^4\mu$$
$$C_b^{w} = - u^4\mu \tag{8}$$

Using the method of initial parameters, the following determinantal frequency equation for the circular arch is obtained

$$\Delta = |a_{iJ}| = 0 \qquad i,J = 1,\ 2,\ 3 \tag{9}$$

where

$$a_{11} = \phi_{44} + C_b^{\varphi} \phi_{34}$$
$$a_{12} = \phi_{45} + C_b^{\varphi} \phi_{35}$$
$$a_{13} = - \phi_{45} - C_b^{\varphi} \phi_{36}$$
$$a_{21} = \phi_{54} - C_b^{w} \phi_{24}$$
$$a_{22} = \phi_{55} - C_b^{w} \phi_{25}$$
$$a_{23} = - \phi_{56} + C_b^{w} \phi_{26}$$
$$a_{31} = \phi_{64} - C_b^{NC} \phi_{34} + C_b^{v} \phi_{14}$$
$$a_{32} = \phi_{65} - C_b^{NC} \phi_{35} + C_b^{w} \phi_{15}$$
$$a_{33} = - \phi_{66} + C_b^{NC} \phi_{36} - C_b^{v} \phi_{16} \tag{10}$$

The functions ϕ_{ik} are given in table 1.

Table 1

Functions ϕ_{ik} for the analysis of vibration of circular arches by the method of initial parameters

i/k	4	5	6
1	$\sum_{j=1,2,3} t_j \frac{\text{sh}\ \lambda_j\ \theta}{\lambda_j}$	$\sum_{j=1,2,3} h_j\ \text{ch}\ \lambda_j\ \theta$	$\sum_{j=1,2,3} h_j \frac{\text{sh}\ \lambda_j\ \theta}{\lambda_j}$
2	$\sum_{j=1,2,3} t_j\ \text{ch}\ \lambda_j\ \theta$	$\sum_{j=1,2,3} h_j\ \lambda_j\ \text{sh}\ \lambda_j\ \theta$	$\sum_{j=1,2,3} h_j\ \text{ch}\ \lambda_j\ \theta$
3	$\sum_{j=1,2,3} t_j\ (1 + \lambda_j^2) \frac{\text{sh}\ \lambda_j\ \theta}{\lambda_j}$	$\sum_{j=1,2,3} t_j\ \text{ch}\ \lambda_j\ \theta$	$\sum_{j=1,2,3} t_j \frac{\text{sh}\ \lambda_j\ \theta}{\lambda_j}$
4	$\sum_{j=1,2,3} t_j\ (1 + \lambda_j^2)\ \text{ch}\ \lambda_j\theta$	$\sum_{j=1,2,3} t_j\ \lambda_j\ \text{sh}\ \lambda_j\ \theta$	$\sum_{j=1,2,3} t_j\ \text{ch}\ \lambda_j\ \theta$
5	$\sum_{j=1,2,3} t_j\ (1 + \lambda_j^2)(\lambda_j^2 + \nu^2 - 1) \frac{\text{sh}\ \lambda_j\ \theta}{\lambda_j}$	$\sum_{j=1,2,3} t_j\ (\lambda_j^6 + \nu^2 - 1)\ \text{ch}\ \lambda_j\ \theta$	$\sum_{j=1,2,3} t_j\ (\lambda_j^2 + \nu^2 - 1) \frac{\text{sh}\ \lambda_j\ \theta}{\lambda_j}$
6	$\sum_{j=1,2,3} t_j\ (\lambda_j^6 + \nu^2\ \lambda_j^2 + c^2)\ \text{ch}\ \lambda_j\ \theta$	$\sum_{j=1,2,3} h_j\ \lambda_j(\lambda_j^6 + \nu^2\ \lambda_j^2 + c^2)\ \text{sh}\ \lambda_j\ \theta$	$\sum_{j=1,2,3} h_j\ (\lambda_j^6 + \nu^2\ \lambda_j^2 + c^2)\ \text{ch}\ \lambda_j\ \theta$

In the table $t_j = h_j(1 + \lambda_3^2)$ $(J = 1,2,3)$, $h_1 = \lambda_3^2 - \lambda_2^2$, $h_2 = \lambda_1^2 - \lambda_3^2$, $h_3 = \lambda_2^2 - \lambda_1^2$ and $c^2 = \nu^2 - u^4 - 1$

3. Numerical analysis

The arches tested were of the same acrylic sheets with $EI_{ab} = 0.03033$ Nm^2 and radii R = 0.5647, 0.6024 m. The values of the critical loads and frequencies depending on the method used are given in tabulated form.

3.1 Oran method

The equations derived by Oran and Reagan (3) were used to find the critical loads and frequencies of the cantilevered arch. The results are given in tabulated form according to the following criteria:

1. (F) Unstable flutter as two roots coalesce
2. (D.I) Unstable divergence with infinitely large frequency
3. (D.II) Unstable divergence with $U_1 = U_2 < 0$

The results are given in table 2.

Critical loading $\bar{\nu}^2$	Frequency u^4
R = 0.5674 m	$\theta_0 = 0.31$
42.567	397.125 (F)
54.65	± 37.82 (D.II)
150.536	∞ (D.I)
R = 0.6024 m	$\theta_0 = 0.38$
28.7	283.59 (F)
37.27	± 71.3 (D.II)
99.80	± 4178.17 (D.II)
99.80	∞ (D.I)

Table 2 Results by Oran method

3.2 Methods of displacement and initial parameters

The results are obtained from the determinantal equation (15) of reference (1).

Case I. The moment of inertia of the nozzle box and it's tip mass offset have been ignored. The results are given in table 3.

Critical loading $\bar{\nu}^2$	Frequency u^4
R = 0.5674 m	θ_0 = 0.31
48.18	183.40 (F)
60.22	74.61 (F)
R = 0.6024 m	θ_0 = 0.38
56.45	68.80 (F)
86.47	151.78 (F)

Table 3 Results by displacement method

Case II. The moment of inertia and the tip mass offset have been accounted for and equation (15) of reference (1) has been used and the results are given in table 4.

Critical loading $\bar{\nu}^2$	Frequency u^4
R = 0.5674 m	θ_0 = 0.31
42.16	14.02 (F)
60.22	74.71 (F)
R = 0.6024 m	θ_0 = 0.38
57.61	68.89 (F)
64.80	87.68 (F)
71.91	91.17 (F)

Table 4. Results by displacement method

Case III.
The mass of the arch has been taken into account and the results are obtained from determinantal equation (9). The results are presented in table 5.

λ_1	λ_2	$\bar{\nu}^2$	u^4
R = 0.5674 m		θ_0 = 0.31	
0.71	4.23	54.20	53.17
1.12	4.23i	42.1	41.29 (D.II)
0.5i	7.03i	42.15	42.19 (D.II)
1.12	3.46i	36	35.31 (D.II)
R = 0.6024 m		θ_0 = 0.38	
1.32i	1.0	54.0559	56.1 (D.II)
1.22i	9.17i	50.452	49.81 (D.II)

Table 5 Results by method of initial parameters

4. Experimental verification

The experimental set up in reference (1) was used to investigate the instability of cantilevered arches with deformation dependent loading. In any experimental work, the study of errors is fundamental and the following factors affected the results:

1. Friction between the plates due to the airbearings was not ac–counted for
2. Coriolis force produced by the water jet from the nozzle box was ignored in the tests
3. Laboratory air pressure was not constant during daytime
4. Water temperature was not constant during the experiments which in turn affected the nozzle box made of hostaline plastic
5. Friction in the pulleys.

With the above restrictions in mind, it is essential to compute the standard deviation for the tests as the tip mass is large in comparison with the mass of the arch. The standard deviation is computed with reference to the results of the massless arch according to the present method and the observed results are given in table 6.

Test No	Q N	Frequency ω	Deviation N
R = 0.5674 m		θ_o = 0.31	
1	4.38	5.03	–0.27
2	4.47	4.63	–0.18
3	4.52	5.03	–0.13
4	5.17	9.26	+0.52
5	4.90	4.71	+0.25
6	4.89	10.05	+0.24
7	4.68	6.28	+0.03
8	4.65	8.36	0
9	4.68	6.28	+0.03
10	4.58	6.28	–0.07
11	4.58	6.28	–0.07
12	4.35	8.98	–0.30
R = 0.6024 m		θ_o = 0.38	
13	5.85	6.28	–0.06
14	5.94	6.28	+0.03
15	5.94	3.96	+0.03

Table 6 Results observed in the tests

Now the standard deviation for the tests is presented in table 7.

Deviation X	No of Deviation	X^2
–0.30	1	0.090
–0.27	1	0.073
–0.18	1	0.032
–0.13	1	0.017
–0.07	2	0.005
0	1	0
+0.03	2	0.001
+0.24	1	0.058
+0.25	1	0.063
+0.52	1	0.270
n = 12	$\Sigma X^2 = 0.615$	

$$S = \sqrt{\frac{\Sigma X^2}{n}} = \sqrt{\frac{0.615}{12}} = 0.20 \text{ N}$$

The standard deviation S is seen to be 0.20 N or about 4 %.

5. Conclusions

The frequency equations for the dynamic instability of cantilevered arches, subjected to configuration dependent loading, are established taking into account the mass of the arch.

The theoretical results obtained is compared with the observed ones. The frequencies obtained differ in some of the results. This is due to the movement restriction of the nozzle box to 2 cm of either side of the neutral position. In Figure 3, the successive positions of the arch is shown at $\bar{\nu}^2 = 64.64$.

Further investigation on the case is a subject of future paper.

Fig. 3 Successive positions of the arch with $\bar{\nu}^2 = 64.64$

ACKNOWLEDGEMENT

The work was supervised by professor Ove Pettersson. Financial support was given by the Department of Fire Safety Engineering.

APPENDIX 1

NOTATIONS

R	radius of arch
EI	flexural rigidity of the arch
p	intensity of pressure
m	uniformly distributed mass of the arch
ω	circular frequency
θ	angular coordinate
$\bar{\omega}$	radial deformation
ν^2	dimensionless quantity defined by equation (2)
$\bar{\nu}^2 = pR^3/EI$	dimensionless follower load
u^4	dimensionless frequency
$\mu = M/mr$	dimensionless mass
$Q = pR$	follower force at the tip of the arch
$C_a^w = \frac{\bar{C}_a^w R^3}{EI}$	dimensionless radial spring constant at end A
$C_b^w = \frac{\bar{C}_b^w R^3}{EI}$	dimensionless radial spring constant at end B
$C_a^v = \frac{\bar{C}_a^v R^3}{EI}$	dimensionless tangential spring constant at end A
$C_b^v = \frac{\bar{C}_b^v R^3}{EI}$	dimensionless tangential spring constant at end B
$C_a^\varphi = \frac{\bar{C}_a^\varphi R}{EI}$	dimensionless rotational spring constant at end A
$C_b^\varphi = \frac{\bar{C}_b^\varphi R}{EI}$	dimensionless rotational spring constant at end B
v_a, v_b	tangential displacements at end A and B, respectively
w_a, w_b	radial displacements at end A and B, respectively
φ_a, φ_b	angular displacements at end and B, respectively
k_1	tangential spring constant at end B
C_o	rotational spring constant at end B

REFERENCES

(1) Arif, G.M. and Pettersson, O., Analytical and Experimental Investigation of Stability of Frames and Arches Subjected to Follower Forces, Proceedings of the 9th International Modal Analysis Conference, Florence, Italy, 1991

(2) Chudnovskii, V.G., Methods of Calculating Vibrations and Stability of Beam and Frame Systems, Kiev, USSR, (in Russian), 1952

(3) Oran, C. and Reagan, R., Buckling of Uniformly Compressed Circular Arches, Journal of the Engineering Mechanics, Irans ASCE EM4, 879–894, 1969

(4) Designers Handbook for Industrial, Apartment, Community Buildings and Houses, Edited by Umanskoff, Izd. Lit. Stoitelstvo, (in Russian), 1973